Journal of Intelligent & Robotic Systems (2020) 98:667–678
https://doi.org/10.1007/s10846-019-01082-2

# Towards Skill Transfer via Learning-Based Guidance in Human-Robot Interaction: An Application to Orthopaedic Surgical Drilling Skill

**Ehsan Zahedi[1] · Fariba Khosravian[2] · Weiqi Wang[2] · Mehran Armand[2] · Javad Dargahi[1] · Mehrdad Zadeh[2]**

Received: 8 June 2018 / Accepted: 21 August 2019 / Published online: 5 November 2019


**Abstract**

This paper presents a machine learning-based guidance (LbG) approach for kinesthetic human-robot interaction (HRI) that can be used in virtual training simulations. Demonstrated positional and force skills are learned to both discriminate the skill levels of users and produce LbG forces. Force information is obtained from virtual forces, which developed based on real computed tomography (CT) data, rather than force sensors. A femur bone drilling simulation is developed to provide a practice environment for orthopaedic residents. The residents are provided with haptic feedback that enable them to feel the variable stiffness of bone layers. The X-ray views of the bone are also presented to them for better tracking of a pre-defined path inside the bone. The simulation is capable of planning a drill path, generating X-rays based on user defined orientation, and recording motion data for user assessment and skill modeling. The knowledge of expert surgeons is also incorporated into the simulation to provide LbG forces for improving the unpredictable motions of the residents. To discriminate the skill level of users, machine learning tools are used to develop surgical expert and resident models. In addition, to improve residents performance, the expert HCRF is used to generate adaptive LbG forces regarding the similarities between residents motions and the expert model. Experimental results show that the learning-based approach is able to assess the skill of users and improve residents performance.

**Keywords** Human-robot interaction · Machine learning-based guidance · Virtual surgical simulation

**JEL Classification** 68T40 · 93C85

## 1 Introduction

Osteoporosis is one of the most common causes for hip fracture, leading to the increase of fracture risk [1]. Even in the developed world, 2% to 8% of males and 9% to 38% of females are diagnosed with osteoporosis [2]. No cure has been developed for osteoporosis, but with proper treatment, the bone loss can be slowed. Since it shows next to no symptoms, most patients do no seek medical attention until bone fracture occurs. Hip fracture is a serious medical issue with a high mortality rate of between 20% and 35% within one year of fractured femur [3, 4].

In osteosynthesis treatment, the surgeons can reposition the dislocated bone fragments into an acceptable position in a non-invasive manner, and apply nails as fixtures. These procedures are guided by real-time x-ray images. Since the surgeon has to determine the depth of the drill by experience, catastrophic results could occur. Thus, developing the intuition for the operation before the surgery is crucial to the success of the operation. This requires excessive practice, which is costly.

Surgical simulations provide a safe environment in which a surgeon may repeatedly practice a procedure without impacting patient safety [5]. The simulations could steepen the initial learning curve and facilitate the transfer of obtained skill to the real clinical environment [6]. Virtual reality (VR) training systems also can serve as safe and effective alternatives to more traditional learning venues, such as the clinical operating room (OR) [7].

✉ Mehrdad Zadeh
mzadeh2@jhu.edu

[1] Department of Mechanical, Industrial, Aerospace Engineering, Concordia University, Montreal, QC, H3G 1M8, Canada

[2] Johns Hopkins University, Baltimore, MD 21218, USA

Training simulators are human-robot interaction (HRI) systems in which robots may assist users to complete a human-robot collaborative manipulation task. Since such systems are human-in-the-loop systems, skill models can be developed and used as references for haptic guidance force calculation in real time. This encourages trainees to correct their motions and improve their performance based on the skill models [8]. Statistical models, e.g. hidden Markov models (HMMs) and their derivatives, have been used to develop surgical skill models for discriminating and evaluating the skill levels of users [9–12]. Using statistical models and machine learning algorithms, the uncertainty of robots and environments are considered for providing sound methodologies in robotics. Statistical models are also highly effective when analytical models are rarely available for complex tasks [13, 14]. In [8], using statistical models, a *kinematic* (positional) learning-based approach has been proposed to generate only guidance forces. However, in the present work a *kinesthetic* (positional and force) learning-based approach is developed for generating guidance forces as well as skill assessment in a virtual surgical simulation.

In HRI, learning from demonstration (LfD) aims to incorporate the knowledge or skills of humans into robot learning [15]. This may enable robots to assist humans for performing collaborative tasks, including lifting objects, manufacturing, and surgical simulations [8]. Demonstrations can be provided through kinesthetic teaching and/or teleoperation [15–17]. In kinesthetic teaching, humans directly guide the robot's body to perform a task while in teleoperation, demonstrations can be done through data gloves [18], motion/vision-based systems [19], or haptic devices [15]. Kinesthetic information have been generated and measured due to a physical interaction with a robot [16, 17, 20] or using haptic devices in teleopration [15]. Similarly, we generate kinesthetic feedback, however, in a surgical virtual simulation based on a developed computed-tomography-based (CT-based) bone model. In addition, virtual fixtures have also been used in haptic-feedback-enabled simulations to improve the execution of demonstrations [21, 22]. On the contrary, in our learning phase (detailed in Section 3), the demonstrations of experts interacting with the simulation, with no virtual fixtures and/or haptic guidance, are used to learn motion stiffness with focus on skill assessment and residents' training/practice.

In the literature, both positional and force data have been used to teach a robot collaborative skills from demonstrations [15, 16, 23, 24]. In orthopedic drilling surgery, since bone tissues have different stiffness, expert surgeons should apply controlled and precise force to each layer of the bone in order to avoid damaging bone tissues. In such applications, the control of interaction force is required to establish an appropriate relationship between applied force by the human/robot and changes in the kinematic state of the contact point with the environment. In contrast to previous work which use expensive force/torque sensors to obtain force skills, we use virtual interaction force to capture force skills for teaching a robot collaborative skills and controlling the interaction force.

In this paper, we propose a learning-based approach in kinesthetic HRI simulation that aims to transfer the skills of expert surgeons to resident trainees (see Fig. 1). During learning phase, the expert demonstrations are used to develop an expert HCRF model for learning the stiffness variations of different bone layers. In addition to the expert HCRF, a novice HCRF model is also developed from the demonstration of novice residents to discriminate the skill levels of a new user. In practice phase, the learning-based approach, which encoded the stiffness variations, guides the trainees to perform training tasks similar to the experts motions.

To investigate our approach, we develop a simulation for femoral bone drilling, with applications to osteonecrosis and fracture stabilization (presented in Section 4). We develop procedures to a) model patient-specific 3D bones from CT scan data, b) incorporate density and stiffness properties into the models for more realistic demonstrations, and c) evaluate residents performance. Our approach is evaluated experimentally, which is detailed in Section 5.

The main contributions of the present work are to a) develop a kinesthetic-HRI-based approach to both discriminate the skill levels of users and generate guidance forces for a virtual surgical simulator, and b) use virtual haptic rendering forces, which are developed based on real CT data, to learn motion stiffness variations.

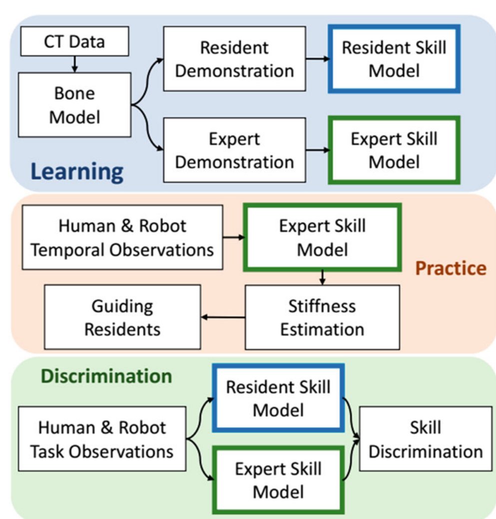


**Fig. 1** Phases of the proposed approach. Learning: use expert and resident demonstrations to develop skill models (HCRFs). Practice: produce real-time learning-based guidance forces to adapt the motion stiffness of residents according to the interaction provided by the experts. Discrimination: assess and discriminate the skill level of user

## 2 General Architecture

The general architecture of the simulation and the learning-based approach is shown in Fig. 2. In LbG, during practice, the expert skill model (HCRF) segments the drilling motion of users within the bone layers. Then, motion similarity estimation block determines how well the current drilling motion of the user is similar to the skill model. The result is used to adapt the value of variable stiffness gains in our learning-based control strategy (variable impedance control block) for producing guidance forces. In this approach, when a user moves the drill less similar to the reference skill model, greater guidance forces are applied to the end-effector and user's hand.

The dynamics of the robot is described by

$$f_H + f_{LbG} + f_{HR} = M\ddot{\boldsymbol{x}} + D\dot{\boldsymbol{x}} \tag{1}$$

where $\boldsymbol{x}$ is the position of the end-effector (drill bit), and $M$ and $D$ are positive-definite matrices representing inertia and damping, respectively. As shown in Fig. 2, the inputs to the robot are human applied force ($f_H$), haptic rendering force ($f_{HR}$), and additional virtual guidance force ($f_{LbG}$), which represents variable guidance force.

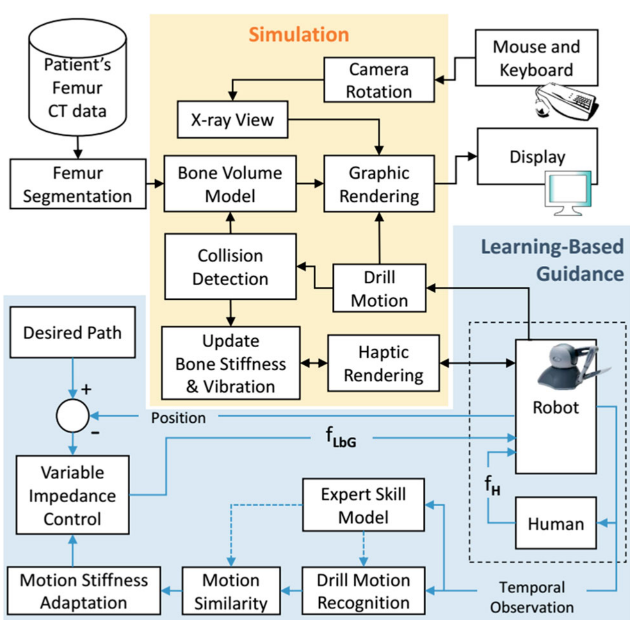


**Fig. 2** General architecture of the simulation and the learning-based guidance (LbG) approach. Expert skill model is used to recognize and segment the drilling motion within the bone layers. Motion similarity generates adaptive stiffness gains ($K_{LbG}$) based on the similarities among current drilling motion and the reference skill model. A variable impedance control strategy calculates forces to guide the user through a reference path. Temporal observations are position, velocity, and acceleration of the robot/human in addition to haptic rendering force

The users may feel two types of haptic force as follows. 1) Haptic force feedback produced to recreate sense of touch for the interaction between drill and the bone in virtual environment. 2) Guidance force that is only applied in practice mode for improving user performance. In the learning phase, for developing skill models (expert and resident models) the guidance force is set to zero to capture the real skill of users.

The inputs of the simulation system are patient specific CT data of femur bone and its segmentation. A semi-automatic segmentation method is used to separate the various layers of the bone: cortical bone, cancellous bone, and bone marrow. The segmented bone data are used to build patient femur model by volume rendering. The density of voxels is assigned regarding to the intensity of pixels in the segmented CT data. The original CT matrix is also preserved for further X-ray simulation. The users are able to rotate the femur model with the mouse and take X-ray from any desired orientation. This results in simulating the actual process in the operation room.

The users interact with the model using a haptic device (Phantom Omni, Geomagic Touch, USA), a keyboard, and a computer mouse. Virtual drill can be manipulated to touch/drill the femur bone model through the stylus of the haptic device. In haptic rendering loop (1000 Hz), the current position and orientation of the haptic stylus are updated for calculating the transformation matrix of the drill as well as collision detection. If a collision between the drill and the bone is detected, force feedback are computed using the transformation matrix and the density of the intersected voxel. In the graphic rendering loop (30 Hz), the existence and intensity of a voxel is updated to generate the view of the bone volume model in the virtual environment (VE).

## 3 Learning-Based Guidance

This section presents the description of the learning-based approach that uses developed skill models to generate adaptive guidance forces and discriminate the skill levels of users. In the proposed approach, an HCRF-based skill model is developed regarding the kinematic data of the expert motions associated with different bone layers. Adaptive guidance forces are generated in real time based on the similarity between the current motion of users and the skill model. Since bone layers have different stiffness, experts adjust drilling forces based on their experiences and skills to operate a smooth drilled path. Similarly, the guidance forces encourage users to follow the target path within the bone with less position error and more similar to the expert motions in terms of velocity, acceleration, and drilling temperature.

### 3.1 Learning-Based Skill Model

Since the analytical models of human motions/behavior are rarely available in HRI applications, the non-linear, non-stationary, and non-deterministic features of stochastic/statistical models make them powerful tools for modeling human behaviors, including the stochastic and uncertain human behavior in terms of both mental state and resulting actions [8, 25]. Stochastic modeling methods (i.e. HCRF) enable machine learning algorithms to 1) capture the spatial and temporal variation of the human motions, 2) capture the change in variance along the movement, and 3) tolerate noise and missing data.

In the present study, we select HCRF to model the sequential motion of human hand and generate guidance forces. HCRF has been successfully used to segment and model sequential data, including spatio-temporal, textual, audio, and visual data [26, 29–31]. In addition, HCRF have been used for many classification applications, including gesture/action recognition [26–29], speech recognition [30], and the classification of transcripts from oral speech [31]. Although HMMs have been used to automatically segment and recognize surgical gestures for surgical skill assessment [9–11], it has been shown that hidden HCRF models can outperform HMMs in terms of user's motion segmentation and generating guidance forces for improving user performance [8].

In order to capture users' sequential dynamic characteristics and segment the drilling motion of a user within different bone layers, we develop an HCRF as a learning-based skill model for the training simulation. Generally the structure of hand motion sequences is complex and statistical models with hidden structures are powerful tools for recognition tasks, including human motion or gesture recognition [26]. In addition, learning-based guidance (i.e. HCRF-based) has shown better user performance improvement, compared to constant haptic guidance [8]. HCRF models incorporate hidden state variables in a discriminative random field model to provide a way to determine a single label for an entire input sequence, e.g. the drilling motion of users. To model the motion of experts within bone layers, an HCRF model is developed by [26]:

$$P(y|O,\theta) = \sum_{S} P(y, S|O,\theta) = \frac{\sum_{S} e^{\psi(y,S,O;\theta)}}{\sum_{y' \in Y, S \in S^m} e^{\psi(y',S,O;\theta)}}, \tag{2}$$

where $y \in Y = \{Cortical\ bone,\ Cancellous\ Bone,\ Bone\ Marrow,\ Necrosis,\ None\}$ is the class label of the drill bit motion in and out of the bone, $O$ is an observation sequence, $S$ is the set of hidden states, and $\theta$ is the model parameters. $\psi(y, S, O; \theta)$, parametrized by $\theta$, calculates the compatibility among a label, a set of observations and hidden states. In order to estimate the parameters, an objective function is utilized as follows [26]:

$$L(\theta) = \sum_{i=1}^{n} log P(y_i|o_i,\theta)) - \frac{1}{2\sigma^2} \|\theta\|^2, \tag{3}$$

where $\{y_i, o_i\}$ is the training set of labeled examples, $n$ is the number of training sequence data, and $\sigma^2$ is the variance of a Gaussian prior. We use a Quasi-Newton optimization method, L-BFGS [32], for finding the optimal parameter values of trained HCRFs ( $\theta^* = \arg\max_\theta\ L(\theta)$).

### 3.2 Adaptive Learning-Based Control

In real time, the proposed learning-based approach recognizes drilling motions and continuously generates motion similarity (*MS*) between the user motion and the trained HCRF:

$$MS(y, O_n) = \arg\max_{y \in Y}\ log\ P(y|O_n, \theta^*) \tag{4}$$

where $O_n$ is the last $n$ observation sequence of user motion.

$P(y|O_n, \theta^*)$ is a probability value that shows how much the current drill motion of the user is similar to the expert motion model. This HCRF-based similarity is used to determine the impedance control gain. An increase in the probability value leads to an increase in motion similarity.

An adaptive learning-based control scheme is used to lessen the effects of unmodeled dynamics, including unobserved deviations from a motion plan, and natural variability of human behavior. Guidance forces are calculated using the following equations:

$$f_{LbG} = -K_{LbG}(MS(y, O_n))[\boldsymbol{x} - \boldsymbol{x}_d] \tag{5}$$

where $f_{LbG}$ is the guidance force, $K_{LbG} > 0$ is an adaptive stiffness gain depends on the motion similarity ($MS$) that is a probability function, $\boldsymbol{x}_d$ is the desired position on the reference path, and $\boldsymbol{x}$ is the current position of the end-effector. The desired position, which is closest to $x$, is instantaneously found based on computational geometry methods [33].

The guidance force is computed using two terms: variable stiffness gain and the position error between the current end-effector position and the desired position. The direction of the guidance force is along with a line, joining the desired position and the current position.

A linear modulation function is selected for $K_{LbG}$ to map each motion similarity value to the corresponding stiffness gain:

$$K_{LbG}(y, O_n) = \frac{K_{max} - K_{min}}{MS_{min} - MS_{max}}(MS(y, O_n) - MS_{max}) + K_{min} \tag{6}$$

where $K_{min}$ and $K_{max}$ are the maximum and minimum stiffness values. The values are selected in order for the safety of haptic device and giving users a good sense of the path they should follow, but they are able to stay outside the reference path, if necessary. $MS_{min}$ and $MS_{max}$, which determine the range of $MS$, are selected based on the results of a pretest user study to minimize motion recognition error rate. This study also indicated that in the operation area of the system, the linear modulation is a fair mapping between $MS$ and $K_{LbG}$ to encourage residents drilling the bone more similar to experts. The stiffness gains are adaptively adjusted in real time according to the end-effector motions.

A windowing approach, in which the last short segments of real-time drill bit motion were sampled ($n$ = *5* data points), was used to compute the motion similarity (*MS*) and guidance forces. Short window sizes may reduce the recognition accuracy of drill motions and accordingly the effectiveness of generated LbG forces. Long window sizes would result in latency and/or mistake in recognizing drill motions while the drill bit enters a bone layer from another one. The window size was experimentally selected to make a balance between these effects. Furthermore, a three-point moving average filter of previous stiffness gain data is used to smooth the stiffness gains and accordingly the guidance forces. The number of points is experimentally selected to obtain a smooth output signal.

According to passivity analysis, which is common for haptic simulations [34, 35], the coupling of the Phantom 1.0 haptic device and a VE is locally stable while the designated stiffness gains keep below 1015 N/m [34]. In this study, although using a different version of Phantom device, we selected a lower range of stiffness in the range 0-222 $N/m$, that was experimentally verified to lead to a stable haptic interaction.

## 4 Femur Bone Drilling Simulation

This section details the development of the simulation. First, we describe the creation of the bone model, which rendered based on patient-specific CT data (Section 4.1). Then, a voxel-based approach is developed to model the different stiffness of bone layers (Sections 4.2 and 4.3). To best of our knowledge, for the first time, we use haptic interaction virtual forces generated in the virtual simulation for developing the skill models, evaluating users' skill, and producing guidance force in a kinesthetic learning-based approach. Next, we present our approach for generating user-defined X-ray views of the bone (Sections 4.5 and 4.6). Finally, the features of the developed graphical user interface are presented (Section 4.7).

### 4.1 Bone Modeling from CT Images

We use CT data of a patient suffering from femoral head necrosis to build a model for the simulation training system. Nowadays, CT and magnetic resonance imaging (MRI) are the two most common modalities that provide 3D medical images. MRI exceeds most in soft-tissue differentiation while CT, a tomography of X-ray by nature, is suited more for bone pathology diagnosis. Both bone density and strength information can be extracted from CT data [36]. We used a set of CT images of a femur bone as the basis of our visual and haptic modeling. The representative sample slices of different view angles and an initial rendering are shown in Fig. 3.

Intensity values on the CT images represent the attenuation coefficient of the tissue. The bright part in the slice is the cortical bone layer whose attenuation coefficient is high, and the dark parts are cancellous bone filled with bone marrow with low attenuations.

We segment the bone by developing a semi-automatic intensity-based thresholding method that requires several thresholds. Although an automatic thresholding method works well in the segmentation of the cortical layer, it often fails to differentiate the bone marrow part from the necrosis part in the femoral head, since in the latter case geometrical information also should be considered. This method includes thresholding; simple region growing algorithm using Robust Statistics Segmentation module in 3D Slicer. After careful adjustment and manual modification, cortical bone layer, femoral head necrosis, and bone marrow in the rest of the cavity are segmented apart and turned into STL (STereoLithography) format surface models (see Fig. 4).

### 4.2 Voxel-Based Rendering

We develop a volume rendering method with respect to bone drilling application and algorithm complexity. Since the tissue of interest is a hard bone, where drilling and tissue removal are the main operations, volume rendering has been preferred since it stores mechanical information at depth of the bone [37–40]. To address algorithm complexity, voxel removal is appropriately modeled in the method with respect to the fact that every voxel has its own density value. When the drilling force is applied on a set of voxels, their densities are reduced by a certain rate, and a voxel will be removed once its density becomes zero. Each voxel is associated with color, surface normal, and density information. The use of voxels also simplifies calculations while identifying interactions with the tool object.

A second rendering method is also developed to produce a more realistic model. To prepare the images for voxel rendering, the top view of the CT data is segmented

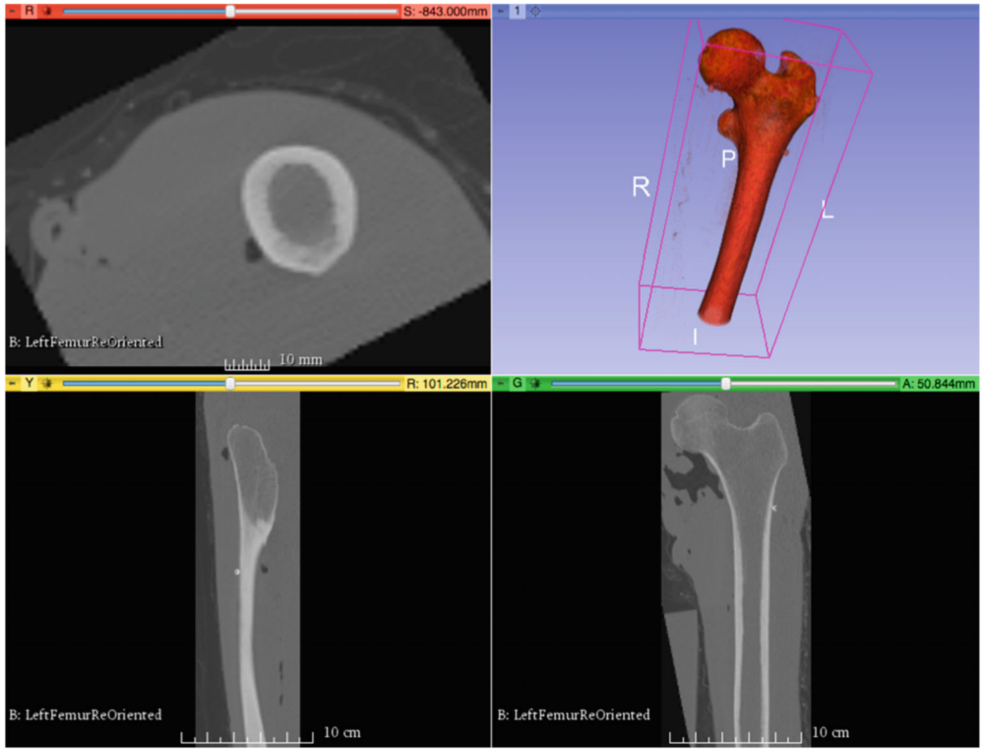


**Fig. 3** CT images as data source for modeling. Upper left: top view; Lower left: left view; Upper right: rendering display; Lower right: front view

to distinguish the bone from the tissue, and remove the tissue from the images. The bone boundaries are identified with respect to the thresholds and filtered out small noise boundaries. Using a built-in colormap, the resulting model consists of voxels which their color values are based on the intensity values from the CT data. In addition, we use surface rendering for haptic display of the tool.

### 4.3 Stiffness Rendering

We consider the mechanical properties of bone layers for developing the simulation. The strength of cortical bone is usually larger than ten times of that of cancellous bone [41]. Brown et al. have studied mechanical property distributions, including stiffness and yield strength distributions, in femur region through direct mechanical measurements [42]. We use their results to adjust the stiffness of the bone layers.

The drilling speed and stiffness of voxel-based objects are completely dependent on the number of voxels that the drill bit is in contact with. However, using a large number of voxels to achieve low drilling speed could place a heavy burden on the graphic processor, as the voxel object would then be exponentially harder to render in the scene. To avoid this conflict, we utilize the color value of each voxel. First, since the application recognizes which voxel of an object is a part of upon contact, a transparency decrement

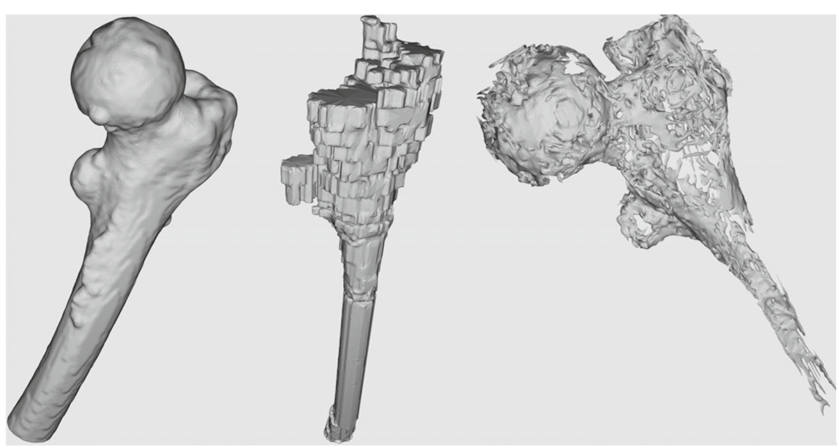

**Fig. 4** Surface models extracted from CT data. From left to right: Cortical bone surface, bone marrow, and necrosis

is set for each object. The value is higher for high density bone and lower for low density bone. Upon contact, the transparency values are extracted from the contacted voxel and decremented by a fix value. Should the transparency value of a voxel reach zero, it is deleted from the scene. Second, the intensity data from the CT scan are used to transfer the different intensity values of the pixels to the transparency values in each voxel. Similar to the first step, decreasing these values at various increments produces the same haptic feedback as drilling through different bone structures.

### 4.4 Drilling Motion

To further enhance the drilling experience, drill vibration is added to the simulation; whenever the drill bit point is in contact with the voxel object and the drilling button of the haptic device is pressed. Each bone layer has its own unique vibration amplitude and frequency. In regard to [40], we set these values so that material with higher stiffness would cause the drill to vibrate at a lower frequency and higher amplitude.

### 4.5 Virtual X-rays

One purpose of this study is to simulate the challenges of actual bone drilling operation. During the surgical treatment of osteonecrosis in OR, surgeons require to stop the drilling and change C-arm position for taking X-rays from different point of views. This assist them to ensure that the drill traverses the correct path within the bone. Our simulation is capable of illustrating the perspective 3D model of the bone as well as three X-ray views of the bone, including front, side, and top. As shown in Fig. 5, these features are simultaneously displayed to users. We use Euler angles to indicate the orientation of our field of view (FOV). The users can change projection direction during drilling. With these X-ray images overlaid with the real-time drill projection, they can locate the 3D drill position, which is critical in actual surgeries.

### 4.6 Mapping Between CT Image and 3D Model

In order to show the right slice of the CT image when moving the plane in space, the relationship between 2D

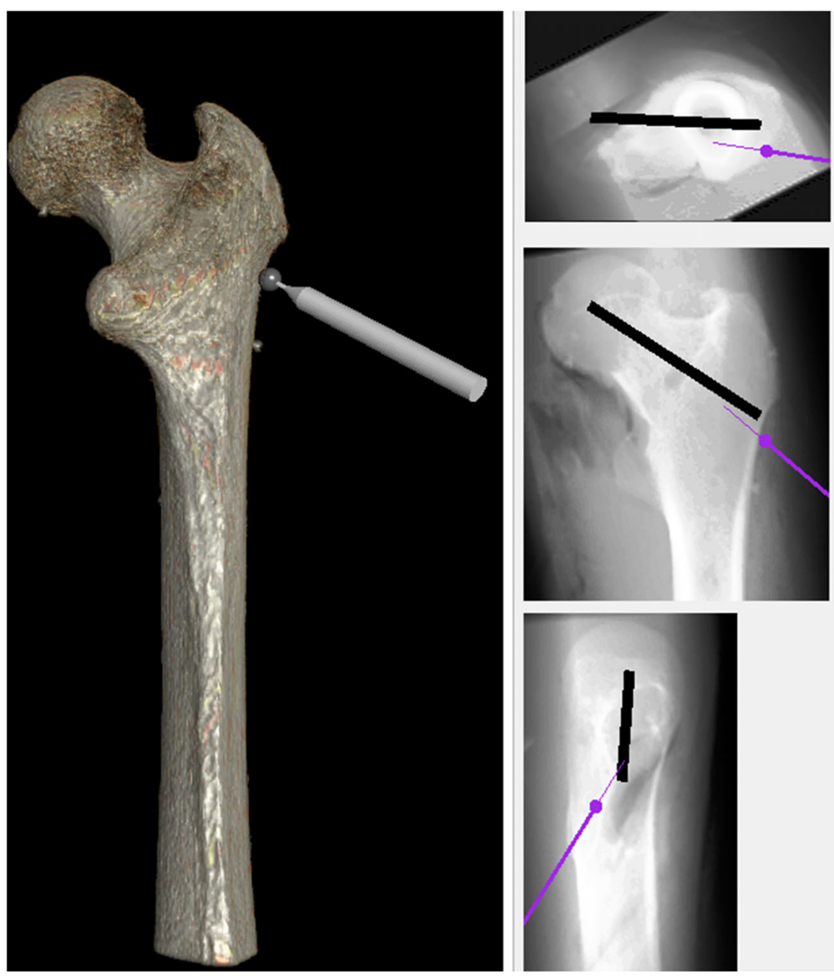

**Fig. 5** To easier perform the drilling task, users are provided with three X-ray views of the bone, the reference trajectory, and a line which shows the direction of the drill

image and 3D model has to be determined. The mapping is based on the number of the slices and the size of the model. If the number of the CT images for front, side, top views are $a, b, c$ ; and the size of the bounding box of the 3D model is $x \times y \times z$; the relationship is expressed as:

$$i = \frac{l}{a} \times x, j = \frac{m}{b} \times y, k = \frac{n}{c} \times z,$$

where $i, j, k$ are the 3D coordinate in world frame correspond to the CT images and $l, m, n$ are the index of the CT images.

### 4.7 Bone Temperature

The simulation also shows the current drill temperature. The bone temperature depends on drilling speed, drilling time or the applied force [43]. For the first time, to best of our knowledge, we simulate drilling bone temperatures, in which the temperature is generated regarding drilling parameters and the experimental data presented in the literature [43]. While the tissue is subject to temperatures more than $60°C$, bone tissue necrosis can be expected [44]. At lower temperatures, injury depends on the drilling time. The bone tissue can bear the temperatures of $45°C$ for more than 600s, $47°C$ for more than 60s and $50°C$ fo more than 30s to prevent thermal necrosis [43].

## 5 Experiment

The goal of this experiment is to investigate the efficacy of the learning-based approach in combination with the developed simulation to discriminate expert surgeons from novice residents and generate guidance forces in practice phase for improving user performance.

### 5.1 Drill Motion Modeling

We train two HCRFs to model the five motions of drilling, the end-effector movement of experts/residents out of the bone (*None*) and within bone layers, including *Cortical Bone, Cancellous Bone, Bone Marrow,* and *Necrosis*. Although expert HCRF is used for generating guidance forces in addition to skill discrimination, resident HCRF is only used to discriminate the skill level of users.

To train the expert HCRF, a data set was gathered from the demonstrations of five expert surgeons who interacted with the simulation through the haptic device and drilled the pre-planned path three times. Figure 6 shows a surgeon while performing a demonstration. Seven surgical residents also demonstrated the task to collect another data set for training the resident HCRF. Observed features included the position of the end-effector as well as the velocity and

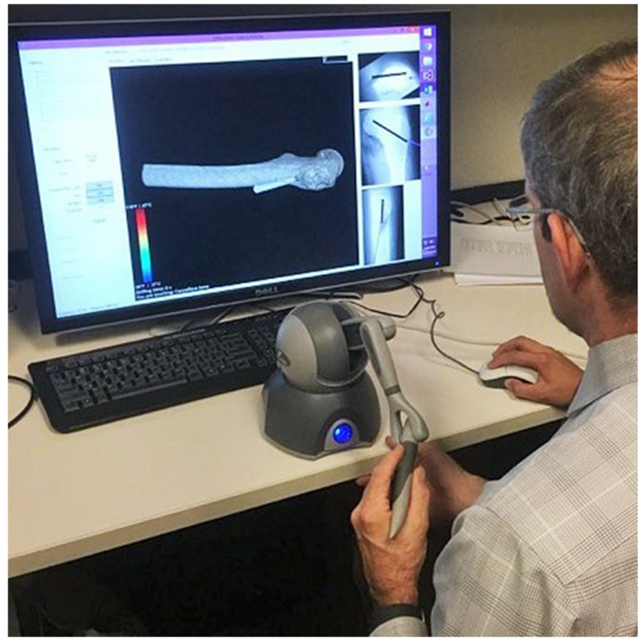

**Fig. 6** An expert surgeon while interacting with the simulation

acceleration, which derived from the position. After the data collection, the data sets were segmented into the five class labels of the drilling motion. The expert and resident HCRFs were developed with 9 states and 12 states, respectively. The number of hidden states were set by minimizing the classification error rate on each training data set. The range of $[MS_{min}, MS_{max}] = [-2500, 0]$ and $[K_{min}, K_{max}] = [0, 250N/m]$ were selected for this experiment regarding the results of a pretest user study.

### 5.2 Procedure

Seven surgical residents (aged 28 to 33 with a mean age of 29.9 years) were asked to complete the task, which was drilling a pre-planed virtual path within the femur bone. We defined the pre-planned path, in which the residents had to pass through all the bone layers to get to the target point. A successful drilling task requires motor skills that improve task performance regarding creating a hole at the correct location without applying excessive force, over-penetration, heating, or skiving with the drill [45].

As shown in Fig. 5, during bone drilling, participants could see the three X-ray views of the bone, the reference trajectory (pre-planned path), and a thin line along the drill that shows the direction of the drill. The reference trajectory is a common drilling path in real surgery [46]. Every participant had five minutes to get familiar with the simulation and then carried out the task three times in the following LbG mode.

**Table 1** Skill Recognition rates (%) based on drill motions

| | Cortical | Cancellous | Marrow | Necrosis | None |
|---|---|---|---|---|---|
| Expert Model | 87.1 | 86.3 | 94.9 | 83.6 | 93.6 |
| Resident Model | 86.1 | 92.8 | 89.5 | 79.6 | 94.0 |

**Learning-based Guidance (LbG)**: The developed expert HCRF model was used to provide adaptive stiffness gains and consequently generate guidance forces.

In the process of data collection for drill motion modeling, five experts and another seven residents had also performed the task, presented in Section 5.1, in the following mode.

**No Guidance (NG)**: No guidance forces was provided to participants. The expert surgeons whose demonstrations are used to develop the expert HCRF are also the same who give the performance parameters of the task. The surgeons performed the task only in NG mode since they were experts in drilling and did not require guidance.

### 5.3 Results and Discussion

We use leave-one-out cross validation method to evaluate the skill discrimination performance of the trained models (expert and resident). We leave one trial of a drill motion out for testing and use the remaining trials for training the drill motion models. Since the collected datasets is not large enough, leave-one-out cross validation is selected for validation. Furthermore, this validation method has been used in the literature to calculate the recognition accuracy of surgical training sub-tasks [47] and residents' level of expertise [48]. The average of classification/recognition results for the two skil models (HCRFs) are presented in Table 1. The average percentage of expert motions that are correctly recognized by the expert model is 89.1%. This rate for the resident model is 88.4%. Considering the recognition of three motion labels out of five for each drilling trial, the skill discrimination of a user as novice-level or expert-level results in 100% correct recognition. Taking into account of all the motion labels during a trial results in the increase of recognition rate to 100%, which is also observed in [10].

To investigate the efficacy of the learning-based approach, we compare the performance of three groups: the five experts who performed the drilling task while no guidance is provided (E-NG), the seven residents who performed the task while LbG is provided (R-LbG), and the other seven residents with no guidance(R-NG). Three metrics are used to evaluate user performance: 1) the completion time of the bone drilling task, 2) the average root mean square error (RMSE) for the position error between the pre-planned path and the drilled path, and 3) the average variation of the bone temperature during the drilling task.

The means and standard errors (SE) of the completion time, position error, and average bone temperature across all participants are presented in Fig. 7. Table 2 shows the between-subject analysis of variance (ANOVA) results, with a rejection level of 0.05. The results of post-hoc Tukey-Kramer pairwise comparisons, $*$ ($P < 0.05$), are shown in Fig. 7. The results show that among the three groups, experts have significantly better performance in terms of completion time and average bone temperature. All the three performances for R-LbG are better than for R-NG. This indicates that providing the guidance forces improves the performance of residents.

The results show that although our learning-based approach results in the improvement of resident performance, residents are not able to perform the task as skillful as the experts. The position error for the experts are not significantly better for R-LbG. The position error depend on the initial alignment of the drill in proper direction while a user starts drilling the bone. While the drill enters the bone, the user has less ability to maneuver the drill. The simulation provides the users with the three X-ray views of the bone to assist them in drilling with more appropriate alignment. This leads to lower RMSE.

Measuring the three metrics enables us not only to assess the skill of users objectively, but discriminate their skill

**Table 2** ANOVA Results for the Performance Metrics. E-NG: experts with no guidance; R-LbG: residents with LbG; R-NG: residents with no guidance; SE: standard error

| Metric | E-NG Mean(SE) | R-LbG Mean(SE) | R-NG Mean(SE) | *F(2,16)* | *P-value* |
|---|---|---|---|---|---|
| Time | 23.29(1.00) | 26.50(0.71) | 30.21(0.98) | 14.92 | < 0.001 |
| RMSE | 5.56(0.54) | 6.59(0.35) | 7.83(0.42) | 6.5 | 0.003 |
| Temp. | 42.41(1.39) | 51.91(1.79) | 58.45(1.92) | 24.35 | < 0.001 |

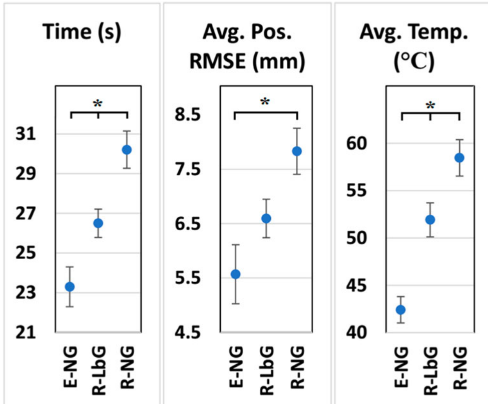


**Fig. 7** Means and standard errors of completion time, average RMSE for position, and average bone temperature across all participants for the three groups: experts with no guidance (E-NG), residents with the proposed guidance (R-LbG), and residents with no guidance (R-NG). The R-LbG group have significantly better time and average temperature compared to R-NG. * marks significant differences

level. The significant difference between the performance of experts and R-NG signifies that in addition to the HCRFs, the metrics can also be used to discriminate the skill level of users as experts or residents.

One idea behind this paper is to investigate if we can manage to improve the performance of the residents for a considered task using machine leaning-based guidance. To achieve this goal, we considered a femur drilling task and measured user performance for each method of providing force. The experiment has been conducted to investigate the performance of the two groups of residents. When force is applied, the performance of the residents significantly improves. However, as the force is not present, the second group of residents is not performing the task as well as the first group provided guidance forces.

One of the contributions of this work is to take the first step in investigating how machine learning-based guidance (LbG) could be used in surgery training by a clinical study. The focus of present work is mostly on studying *performance* not *learning effect*. Similarly, many researchers have been evaluated such learning-based (LfD-based) approaches only by investigating user/task performance [8, 16, 17].

## 6 Conclusion

This paper presented a learning-based approach that aims to learn robots for transferring skills from expert to trainees. We developed the approach for both skill discrimination and user performance improvement in a virtual reality (VR) simulation for femur drilling surgery. Real CT data were used to provide the users with the feeling of bone stiffness variations in regard to the drilled depth. HCRF-based skill models (expert HCRF and resident HCRF) were developed from experts and residents demonstrations to segment the drill motion within different bone layers as well as differentiate user's skill as experts or residents. In practice phase, the expert HCRF was used to adapt motion stiffness and generate learning-based guidance (LbG) for assisting residents with applying appropriate forces within different bone layers. A set of performance metrics was also used to objectively evaluate the skills of users.

The experimental results of our clinical study showed that LbG significantly improves residents performance in terms of completion time and average bone temperature. However, the residents were not able to perform a drilling task in a similar skill level of the experts. The results also indicated that in addition to skill models, performance metrics, including task completion time, RMSE for position, and average bone temperature, can be used to discriminate the skill levels of users.

In future work, the learning effects of the proposed LbG will be studied. In addition, a 6 DoF haptic devices will be used to provide more realistic virtual simulation.

**Acknowledgements** We thank Russell H. Taylor for facilitating this research in the LCSR lab at Johns Hopkins University.

## References

1. Schapira, D., Schapira, C.: Osteoporosis: the evolution of a scientific term. Osteoporos. Int. **2**(4), 164 (1992)
2. Wade, S., Strader, C., Fitzpatrick, L., Anthony, M., O'Malley, C.: Estimating prevalence of osteoporosis: examples from industrialized countries. Arch. Osteoporos. **9**(1), 182 (2014)
3. Goldacre, M.J., Roberts, S.E., Yeates, D.: Mortality after admission to hospital with fractured neck of femur: database study. Bmj **325**(7369), 868 (2002)
4. Thorngren, K.G.: National Registration of Hip Fractures (2008)
5. Coles, T., Meglan, D., John, N.: The role of haptics in medical training simulators : a survey of the state of the art. IEEE Trans. Haptic **4**(1), 51 (2011)
6. Ahlberg, G.: The role of simulation technology for skills acquisition in image guided surgery. Institutionen för kirurgisk vetenskap/Department of Surgical Science (2005)
7. Seymour, N.: VR To OR: a review of the evidence that virtual reality simulation improves operating room performance. World J. Surg. **32**(2), 182 (2008)
8. Zahedi, E., Dargahi, J., Kia, M., Zadeh, M.: Gesture-based adaptive haptic guidance: a comparison of discriminative and generative modeling approaches. IEEE Robotics and Automation Letters **2**(2), 1015 (2017)
9. Rosen, J., Brown, J., Chang, L., Sinanan, M., Hannaford, B.: Generalized approach for modeling minimally invasive surgery as a stochastic process using a discrete Markov model. IEEE Trans. Biomed. Eng. **53**(3), 399 (2006)
10. Reiley, C., Hager, G.: Task versus subtask surgical skill evaluation of robotic minimally invasive surgery. Medical Image Computing and Computer-Assisted Intervention (MICCAI), pp. 435–442 (2009)

11. Kahol, K., Vankipuram, M., Smith, M.: Cognitive simulators for medical education and training. J. Biomed. Inform. **42**(4), 593 (2009)
12. Chi, W., Rafii-Tari, H., Payne, C.J., Liu, J., Riga, C., Bicknell, C., Yang, G.Z.: A learning based training and skill assessment platform with haptic guidance for endovascular catheterization. In: IEEE International Conference on Robotics and Automation (ICRA), pp. 2357–2363, IEEE (2017)
13. Lee, D., Ott, C.: Incremental kinesthetic teaching of motion primitives using the motion refinement tube. Auton. Robot. **31**(2-3), 115 (2011)
14. Medina, J., Lee, D., Hirche, S.: Risk-Sensitive Optimal feedback control for haptic assistance. In: IEEE International Conference on Robotics and Automation (ICRA), pp. 1025–1031 (2012)
15. Rozo, L., Jiménez, P., Torras, C.: A robot learning from demonstration framework to perform force-based manipulation tasks. Intell. Serv. Robot. **6**(1), 33 (2013)
16. Rozo, L., Calinon, S., Caldwell, D.G., Jimenez, P., Torras, C.: Learning physical collaborative robot behaviors from human demonstrations. IEEE Trans. Robot. **32**(3), 513 (2016)
17. Kronander, K., Billard, A.: Learning compliant manipulation through kinesthetic and tactile human-robot interaction. IEEE Trans. Haptic **7**(3), 367 (2014)
18. Bernardino, A., Henriques, M., Hendrich, N., Zhang, J.: Precision grasp synergies for dexterous robotic hands. In: IEEE International Conference on Robotics and Biomimetics (ROBIO), pp. 62–67 (2013)
19. Calinon, S., Billard, A.: Incremental learning of gestures by imitation in a humanoid robot. In: Proceedings of the ACM/IEEE international conference on Human-robot interaction, pp. 255–262 (2007)
20. Cha, E., Kronander, K., Billard, A.: Combined kinesthetic and simulated interface for teaching robot motion models. In: IEEE International Symposium on Robot and Human Interactive Communication (RO-MAN), pp. 83–88 (2015)
21. Aleotti, J., Caselli, S., Reggiani, M.: Leveraging on a virtual environment for robot programming by demonstration. Robot. Auton. Syst. **47**(2), 153 (2004)
22. Aleotti, J., Caselli, S., Reggiani, M.: Evaluation of virtual fixtures for a robot programming by demonstration interface. IEEE Trans. Syst. Man Cybern. Part A Syst. Hum. **35**(4), 536 (2005)
23. Koropouli, V., Lee, D., Hirche, S.: Learning interaction control policies by demonstration. In: IEEE/RSJ International Conference on Intelligent Robots and Systems (IROS), pp. 344–349 (2011)
24. Kormushev, P., Calinon, S., Caldwell, D.G.: Imitation learning of positional and force skills demonstrated via kinesthetic teaching and haptic input. Adv. Robot. **25**(5), 581 (2011)
25. Medina, J., Lorenz, T., Hirche, S.: Synthesizing anticipatory haptic assistance considering human behavior uncertainty. IEEE Trans. Robot. **31**(1), 180 (2015)
26. Wang, S., Quattoni, A., Morency, L., Demirdjian, D., Darrell, T.: Hidden conditional random fields for gesture recognition. 2006 IEEE Computer Society Conference on Computer Vision and Pattern Recognition **2**, 1521 (2006)
27. Lu, W., Tong, Z., Chu, J.: Dynamic hand gesture recognition with leap motion controller. IEEE Signal Process Lett. **23**(9), 1188 (2016)
28. Arzani, M.M., Fathy, M., Aghajan, H., Azirani, A.A., Raahemifar, K., Adeli, E.: Structured prediction with short/long-range dependencies for human activity recognition from depth skeleton data. In: IEEE/RSJ International Conference on Intelligent Robots and Systems (IROS), pp. 560–567 (2017)
29. Liu, A.A., Nie, W.Z., Su, Y.T., Ma, L., Hao, T., Yang, Z.X.: Coupled hidden conditional random fields for rgb-d human action recognition. Signal Process. **112**, 74 (2015)
30. Hong, W.T.: HCRF-Based model compensation for noisy speech recognition. In: IEEE International Symposium on Consumer Electronics (ISCE), pp 277–278 (2013)
31. Barriere, V., Clavel, C., Essid, S.: Opinion dynamics modeling for movie review transcripts classification with hidden conditional random fields. arXiv:1806.07787 (2018)
32. Nocedal, J., Wright, S.: Numerical optimization. Springer Science & Business Media (2006)
33. Smid, M.: Handbook of computational geometry (2000)
34. Diolaiti, N., Niemeyer, G., Barbagli, F., Salisbury, J.K.: Stability of haptic rendering: Discretization, quantization, time delay, and coulomb effects. IEEE Trans. Robot. **22**(2), 256 (2006)
35. Adams, R.J., Hannaford, B.: Stable haptic interaction with virtual environments. IEEE Trans. Robot. Autom. **15**(3), 465 (1999)
36. Teo, J.C., Si-Hoe, K.M., Keh, J.E., Teoh, S.H.: Relationship between ct intensity, micro-architecture and mechanical properties of porcine vertebral cancellous bone. Clin. Biomech. **21**(3), 235 (2006)
37. Sofronia, R.E., Davidescu, A., Savii, G.G.: Towards a virtual reality simulator for orthognathic basic skils. In: Applied Mechanics and Materials, vol. 162, pp. 352–357 (2012)
38. Bogoni, T.N., Pinho, M.S.: Haptic technique for simulating multiple density materials and material removal. In: International Conference on Computer Graphics Visualization and Computer Vision, pp. 151–160 (2013)
39. Liu, Y., Laycock, S.D.: A haptic system for drilling into volume data with Polygonal Tools. In: TPCG, pp. 9–16 (2009)
40. Morris, D., Sewell, C., Blevins, N., Barbagli, F., Salisbury, K.: A collaborative virtual environment for the simulation of temporal bone surgery. In: International Conference on Medical Image Computing and Computer-Assisted Intervention, pp. 319–327 (2004)
41. Müller, M.E., Allgöwer, M., Perren, S.: Manual of Internal Fixation: Techniques Recommended by the AO-ASIF Group. Springer Science & Business Media, Berlin (1991)
42. Brown, T.D., Ferguson, A.B.: Mechanical property distributions in the cancellous bone of the human proximal femur. Acta Orthop. Scand. **51**(1-6), 429 (1980)
43. Pandey, R.K., Panda, S.: Drilling of bone: a comprehensive review. Journal of Clinical Orthopaedics and Trauma **4**(1), 15 (2013)
44. Boner, V., Kuhn, P., Mendel, T., Gisep, A.: Temperature evaluation during pmma screw augmentation in osteoporotic bone—an in vitro study about the risk of thermal necrosis in human femoral heads. J. Biomed. Mater. Res. B Appl. Biomater. **90**(2), 842 (2009)
45. Pourkand, A., Salas, C., Regalado, J., Bhakta, K., Tufaro, R., Mercer, D., Grow, D.: Objective evaluation of motor skills for orthopedic residents using a motion tracking drill system: Outcomes of an abos approved surgical skills training program. Iowa Orthop. J. **36**, 13 (2016)
46. Pettersson, J., Palmerius, K.L., Knutsson, H., Wahlstrom, O., Tillander, B., Borga, M.: Simulation of patient specific cervical hip fracture surgery with a volume haptic interface. IEEE Trans. Biomed. Eng. **55**(4), 1255 (2008)
47. Reiley, C.E., Plaku, E., Hager, G.D.: Motion generation of robotic surgical tasks : learning from expert demonstrations. Engineering in Medicine and Biology Society, pp. 967–970 (2010)
48. Chmarra, M.K., Klein, S., de Winter, J.C., Jansen, F.W., Dankelman, J.: Objective classification of residents based on their psychomotor laparoscopic skills. Surg. Endosc. **24**(5), 1031 (2010)


**Publisher's Note** Springer Nature remains neutral with regard to jurisdictional claims in published maps and institutional affiliations.

**Ehsan Zahedi, Ph.D** is currently a research scientist at Stradigi AI, where he is applying machine learning approaches to real industrial problems. He received his PhD in Mechanical Engineering from Concordia University, Montreal, Canada. Towards working for his PhD, he had the opportunity to collaborate with researchers at Johns Hopkins University as a visiting scholar. His research experiences and interests lie at the intersection of machine learning, haptics, control systems, and robotics. His doctoral research contributions have been concentrated to design and develop adaptive haptic guidance approaches using machine learning algorithms for human-robot interaction (HRI). The main goal of the research is to capture underlying human skills from demonstrations to develop learning-based approaches that aim to transfer the skill of experts to trainees in HRI.

**Fariba Khosravian** is currently a developer for online haptic educational modules at Tech Training Zone. As a team member, she has collaborated with several researchers to conduct a research project on developing a haptic-enabled surgical simulator for training surgical residents using learning-based haptic guidance in human-robot interaction. A femur bone drilling simulation is developed to provide a practice environment for orthopaedic residents. The residents are provided with haptic feedback that enable them to feel the variable stiffness of bone layers. She was a graduate assistant at REACH lab and received his master of engineering at 2012 in Computer Engineering from Kettering University. Fariba has also over 6 years of experience as an engineer and software developer specialist. She is interested largely in the areas of haptics, physical human robot interaction (pHRI), and medical Robotics.

**Weiqi Wang** is a software engineer at INNFOS, a robotics R&D company, where he is developing control algorithms for humanoid and quadrupedal service robots to make human-machine interactions safer and more intelligent. He received his master degree in Mechanical Engineering from Johns Hopkins University. His research interests include haptics, robotics, locomotion and computer vision. Currently , his research involves the adaptation of unpredictable environment for legged robots and robotic arms.

**Mehran Armand, Ph.D** received the Ph.D. degree in mechanical engineering and the Ph.D. degree in kinesiology both from the University of Waterloo, ON, Canada, with a focus on bipedal locomotion. He is currently a Principal Scientist and holds joint appointments with Departments of Mechanical Engineering and Orthopaedic Surgery, Johns Hopkins University (JHU). Prior to joining JHU/Applied Physics Laboratory in 2000, he completed Postdoctoral fellowships at JHU Orthopaedic Surgery and Otolaryngology-Head and Neck Surgery. He currently directs the collaborative Laboratory for Biomechanical and Image-Guided Surgical Systems, Laboratory for Computational Sensing and Robotics, JHU/Whiting School of Engineering.

**Javad Dargahi, Ph.D** is a professor in the Mechanical, Industrial and Aerospace Engineering Department of Concordia University. He received his B.Sc. and M.Sc. in Mechanical Engineering from UK, and his Ph.D. degree from Glasgow Caledonian University in the area of “Robotic tactile sensing”. He was a Senior Post-Doctoral Research Associate with the Micromachining/Medical Robotics Group at Simon Fraser University. His research area includes: Design and fabrication of haptic sensors and feedback systems for minimally invasive surgery and robotics. Dr. Dargahi has developed innovative methods of implementing mechatronics in medicine and has written a book with the title of “Mechatronics in Medicine”. He has authored over 180 journal and conference articles, three books published by McGraw-Hill and Wiley, and two patents in the area of his research. One of his books “Artificial Tactile Sensing in Biomedical Engineering” was the runner-up for the prestige PROSE award, considered as Oscars of the Association of American Publishers. Professor Dargahi was a principal reviewer of several major NASA proposals in the area of “Crew health and performance in space exploration mission”. Dr. Dargahi is among the 10 top university professors in Montreal that recently received a major research and training initiative by the federal funding agency.

**Mehrdad H. Zadeh, Ph.D** is an associate professor and an advisor of AutoDrive Challenge$^{TM}$ competition at Kettering University, MI. From Sept. 2015 to January 2017, he served as a visiting associate professor at Johns Hopkins University, Laboratory for Computational Sensing + Robotics (LCSR), MD, where he collaborates on the design and development of haptic-enabled surgical simulation. He received his M.A.Sc. (2004) and Ph.D (2009) in Electrical and Computer Engineering from Concordia University and the University of Waterloo, Canada, respectively. He also has over 8 years of industry experience as an engineer and software development specialist. He is interested largely in the areas of autonomous systems, haptics, physical human robot interaction (pHRI), and Robotics.